Optimized Merger of Ocean Chlorophyll Algorithms of MODIS-Aqua and VIIRS

Mati Kahru, Raphael M. Kudela, Clarissa R. Anderson, and B. Greg Mitchell

***Abstract*—Standard ocean chlorophyll-a (Chla) products from currently operational satellite sensors Moderate Resolution Imaging Spectroradiometer (MODIS) Aqua and Visible Infrared Imager Radiometer Suite (VIIRS) underestimate medium and high *in situ* Chla concentrations and have approximately 9% bias between each other in the California Current. By using the regional optimization approach of Kahru *et al.*, we minimized the differences between satellite estimates and *in situ* match-ups as well as between estimates of the two satellite sensors and created improved empirical algorithms for both sensors. The regionally optimized Chla estimates from MODIS-Aqua and VIIRS have no bias between each other, have improved retrievals at medium to high *in situ* Chla, and can be merged to improve temporal frequency and spatial coverage and to extend the merged time series.**

***Index Terms*—Chlorophyll, Moderate Resolution Imaging Spectroradiometer (MODIS), ocean color, phytoplankton, Visible Infrared Imager Radiometer Suite (VIIRS).**

I. Introduction

COMBINING or merging data from multiple sensors is required to improve the temporal resolution and spatial coverage of ocean color imagery and to construct long time series or climate data records using data from multiple sensors [2]–[5]. Currently (i.e., in mid-2015), there are two well-calibrated global ocean color sensors in operation: Moderate Resolution Imaging Spectroradiometer on Aqua (MODISA) and Visible Infrared Imaging Radiometer Suite (VIIRS) on Suomi NPP. While improvements in on-orbit sensor calibration [6] have greatly improved the compatibility between data from different sensors, significant differences remain [7], [8]. Moreover, global algorithms may not be regionally optimal as significant differences exist in bio-optical properties of different oceanic provinces [9]. Standard NASA ocean chlorophyll-a (Chla) algorithms significantly underestimate *in situ* values in the California Current at high concentrations, often by a factor of 5 [1]. This is highly relevant for detection and monitoring of phytoplankton blooms, including harmful algal blooms [10]. While differences between Chla estimates from MODIS-Aqua and VIIRS have diminished after multiple reprocessings, they still exist [8].

Kahru *et al.* [1] created optimized empirical algorithms for the California Current for a suite of four sensors (OCTS, SeaWiFS, MERIS, and MODISA) and the time period of 1997–2011. An update to that work is currently needed as 1) MERIS stopped operating in April 2012; 2) new data from VIIRS are available from the beginning of 2012; and 3) both MODISA and VIIRS data have been reprocessed by NASA's Ocean Biology Processing Group. The purpose of this work is to create empirical algorithms that are optimized for creating a merged Chla time series in the California Current for the period of 2012–2015 from the two currently available sensors MODISA and VIIRS.

II. Data and Methods

We used *in situ* Chla data collected by the California Cooperative Oceanic Fisheries Investigations (CalCOFI) on their quarterly cruises covering a regular grid of stations from nearshore to as far as 600 km offshore for the entire coast of California [11]. In total, 3388 near-surface Chla samples from 2002–2014 were used to validate MODISA data, and 744 Chla samples from 2012–2014 were used to validate VIIRS data.

All satellite data were acquired at level 2 (i.e., processed to surface quantities but unmapped) with approximately 1-km ground resolution. MODISA (2002–2014, version 2013.1.1) and VIIRS (2012–2014, version 2014.0.1) level-2 data were obtained from NASA's Ocean Color Web (http://oceancolor.gsfc.nasa.gov/). The standard NASA Chla algorithm uses empirical polynomial fits between satellite-derived maximum band ratio (MBR) of remote sensing reflectance (Rrs) bands and near-surface Chla [12] with the coefficient values for each sensor given at http://oceancolor.gsfc.nasa.gov/cms/atbd/chlor_a.

The validation of satellite products using quasi-simultaneous and spatially collocated measurements (match-ups) of satellite and *in situ* data followed the procedures of previous studies [1], [8], [13], [14]. We assumed that the following level-2 flags made a pixel invalid: ATMFAIL, LAND, HISATZEN, STRAYLIGHT, CLDICE, CHLFAIL, SEAICE, NAVFAIL, and HIPOL (see http://oceancolor.gsfc.nasa.gov/VALIDATION/flags.html for an explanation of the flags). All variables in the level-2 files were extracted from a 3 × 3-pixel window centered at the pixel nearest to the *in situ* sample. For statistical analysis, we accepted only those match-ups with at least five

Manuscript received May 28, 2015; revised July 9, 2015; accepted August 17, 2015. Date of publication September 7, 2015; date of current version October 27, 2015. This work was supported by the NASA Ocean Biology and Biogeochemistry Program Grants NNX09AT01G (M. Kahru and R. M. Kudela), NNX13AL28G (C. R. Anderson, R. M. Kudela, and M. Kahru), and NNX14AC42G (C. R. Anderson and R. M. Kudela) and by the National Science Foundation (Grant OCE-1026607 to the CCE-LTER Program).

M. Kahru and B. G. Mitchell are with Scripps Institution of Oceanography, University of California, San Diego, La Jolla, CA 95064 USA (e-mail: mkahru@ucsd.edu; gmitchell@ucsd.edu).

R. M. Kudela and C. R. Anderson are with the Ocean Sciences Department, University of California, Santa Cruz, Santa Cruz, CA 95064 USA (e-mail: kudela@ucsc.edu; clrander@ucsc.edu).

Color versions of one or more of the figures in this paper are available online at http://ieeexplore.ieee.org.

Digital Object Identifier 10.1109/LGRS.2015.2470250

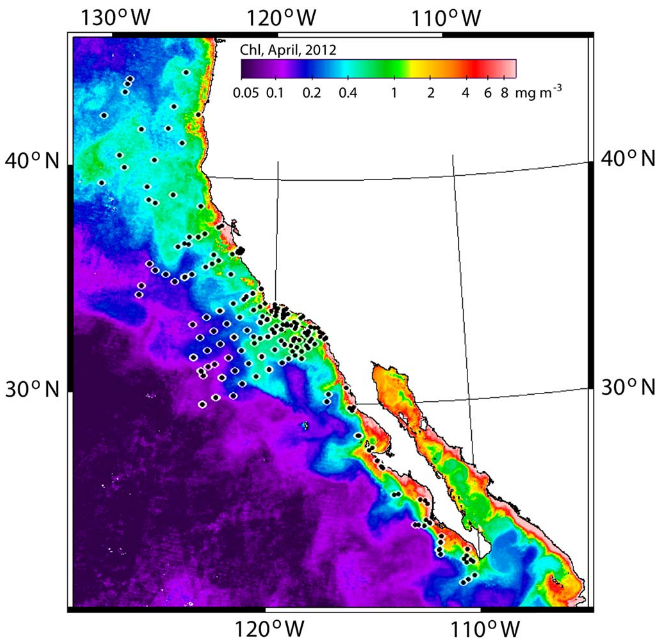

Fig. 1. Locations of the MODIS-Aqua Chla match-ups (black dots with white circles) within 3-h time difference overlaid on the April 2012 Chla composite.

valid pixels (out of nine). The maximum temporal difference between satellite and *in situ* measurements was set at 3 h. Satellite match-ups with high variability within the 3 × 3-pixel window were excluded if $(\text{Max} - \text{Min})/\text{Min} > 0.6$ for the standard Chla variable *chlor_a*. The arithmetic mean Chla value of all valid pixels within the 3 × 3-pixel window was used as the satellite retrieval. The spatial distribution of MODISA match-ups with *in situ* measurements of Chla is shown in Fig. 1.

Satellite-derived Rrs values between different sensors are difficult to compare at level 2, i.e., without remapping to a common map. Although both MODISA and VIIRS have equatorial crossing times at approximately 1:30 P.M., their pixel-to-pixel comparison at a spatial resolution of $\sim$1 km^2 corresponding to their level-2 data shows high variability [8]. We therefore used spatially binned and averaged Rrs values over a grid of 1° latitude × 1° longitude covering an approximately 1000-km-wide area along the coast extracted from daily NASA level-3 datasets. Those daily mean Rrs values of MODISA and VIIRS were then matched with each other. In order to eliminate cloud edges and coastal zones, we kept only those matching Rrs pairs with at least 99% of the pixels within each 1° × 1° subarea having valid values. As a result, a total of 4060 matching Rrs vectors for MODISA and VIIRS were found for the period of 2012–2014. These MODISA to VIIRS match-ups were then used in the minimization of the differences in the Chla algorithm between MODISA and VIIRS.

Several statistical measures were used to assess the performance of satellite products against *in situ* observations and between different satellite sensors. For satellite to *in situ* match-ups, we assume that O_i is the ith observation of an *in situ* variable and P_i is the corresponding predicted satellite variable. For sensor-to-sensor match-ups, the choice of the observed *versus* predicted variable is arbitrary, but we used MODISA estimates as O_i. As an estimate of the prediction scatter, we

TABLE I

STATISTICS FOR MATCH-UPS OF THE NASA STANDARD *chlor_a* PRODUCT WITH *IN SITU* CHLA WITH UP TO 3-h TIME DIFFERENCE AND AT LEAST FIVE VALID PIXELS. N = NUMBER OF MATCH-UPS, R^2 = COEFFICIENT OF DETERMINATION, MDAPE = MEDIAN ABSOLUTE PERCENT ERROR, MDRPE = MEDIAN RELATIVE PERCENT ERROR, RMSE = ROOT MEAN SQUARE ERROR, AND RMASLOPE = SLOPE OF THE RMA LINEAR REGRESSION

Sensor	N	R^2	MdAPE	MdRPE	RMSE	RmaSlope
MODISA	306	0.87	22.5	−0.1	0.15	0.88
VIIRS	74	0.85	31.0	8.0	0.21	0.68

used the median absolute percentage error (MdAPE), which was calculated as $\text{MdAPE} = 100 \times \text{median}\ (|(P_i - O_i)/O_i|)$. For comparing two sensors, we used the median unbiased absolute percentage error (MdUAPE), which was calculated as $\text{MdUAPE} = 100 \times \text{median}\ (|(P_i - O_i)/[0.5^*(P_i + O_i)]|)$. As an estimate of bias, we used the median relative percentage error (MdRPE), which was calculated as $\text{MdRPE} = 100 \times \text{median}\ ((P_i - O_i)/O_i)$. These statistics were calculated for P_i and O_i using untransformed values (i.e., not $\log_{10}$). We also include the coefficient of determination (R^2), the slope of the reduced major axis (RMA) regression, and the root-mean-square error (rmse), all calculated on $\log_{10}$-transformed variables.

III. RESULTS

A. Match-Ups With Standard chlor_a Products

Satellite to *in situ* match-ups of Chla using the NASA standard *chlor_a* product over three orders of magnitude (Fig. 2 and Table I) have relatively high coefficients of determination ($R^2 = 0.87$ for MODISA and 0.85 for VIIRS) but also show bias. For example, all MODISA match-ups with *in situ* Chla > 2 mg m^{-3} underestimate *in situ* Chla. For VIIRS, the standard *chlor_a* product suffers from overestimation at low *in situ* Chla and underestimation at medium and high Chla, which causes the slope of the RMA regression to be significantly less than one (0.68; Table I).

B. Optimized MBR Algorithm

Standard empirical ocean color algorithms OC3 and OC4 [12] use polynomial fits between $\log_{10}$-transformed *in situ* Chla (Cins) and $\log_{10}$-transformed MBR of Rrs measured *in situ*. MBR is calculated as the maximum of Rrs at two or more wavelengths (e.g., $Rrs443$ and $Rrs488$ for MODISA or $Rrs443$ and $Rrs486$ for VIIRS) to the Rrs of the green band ($Rrs547$ for MODISA and $Rrs551$ for VIIRS). In order to remove the bias evident in Fig. 2, we created our own best fits to the match-up points. The distribution of match-up points is highly uneven as there are more points in the middle of the range than at both ends of the distribution. To reduce the effect of the uneven distribution, the match-up points were aggregated into bins by using the median values of small brackets of $\log_{10}(\text{Cins})$ and the corresponding medians of $\log_{10}(\text{MBR})$ following [3] and binning interval of 0.04 in $\log_{10}(\text{MBR})$ units.

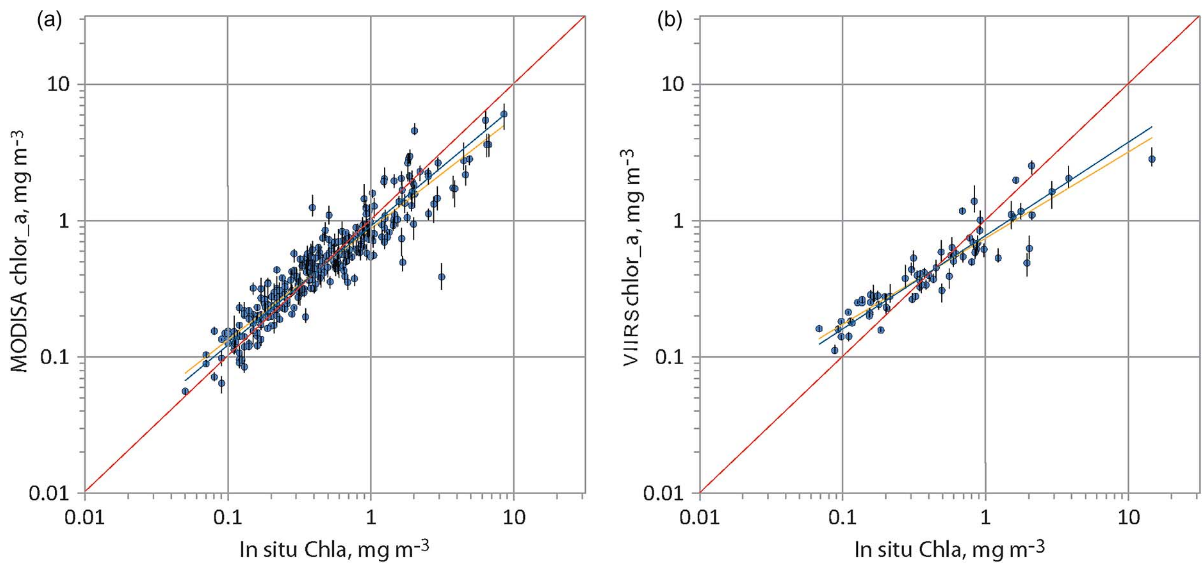

Fig. 2. Chlorophyll-a match-ups with (a) MODISA and (b) VIIRS using standard NASA *chlor_a* products. The red line is the one-to-one line, and the blue line is the RMA linear regression.

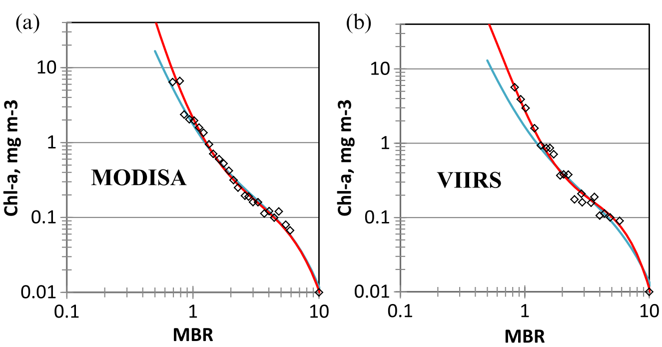

Fig. 3. Optimized Chla algorithm (red) compared to standard NASA OC3 (blue) and bracket points of *in situ* Chla match-ups (black diamonds) as a function of the MBR of remote sensing reflectance for (a) MODISA and (b) VIIRS.

TABLE II

STATISTICS OF VIIRS VERSUS MODISA COMPATIBILITY WITH DIFFERENT ALGORITHMS: STANDARD NASA OC3 *chlor_a*, EMPIRICAL FIT TO *IN SITU* CHLA MATCH-UPS, AND THE OPTIMIZED CHLA ALGORITHM. THE STATISTICS WITH SIGNIFICANT IMPROVEMENT ARE SHOWN IN BOLD

Algorithm	R^2	MdAPE, %	MdRPE, %	RMSE	RmaSlope
Standard	0.95	**13.7**	**-9.4**	0.105	1.04
In situ fit	0.94	**14.0**	**-6.8**	0.125	1.12
Optimized	0.95	**10.3**	**-0.1**	0.113	1.04

TABLE III

POLYNOMIAL COEFFICIENTS OF THE OPTIMIZED CHLA ALGORITHM (CALFIT2015) FOR MODISA AND VIIRS

Sensor	***a0***	***a1***	***a2***	***a3***	***a4***
MODISA	0.327711	-3.44875	3.031143	-0.42728	-1.45675
VIIRS	0.442695	-3.65908	2.31464	2.369933	-3.41648

The resulting "bracket" points (24 for MODISA and 20 for VIIRS) were then used in algorithm development (Fig. 3).

Ideally, by "tuning" the algorithms of multiple sensors to the same set of *in situ* data, the resulting estimates by different sensors should be compatible between each other. In reality, as the Chla high end is poorly constrained due to few scattered match-ups, the resulting empirical algorithms do not improve the intersensor consistency and may even make it worse [1]. Indeed, as the main difference of the empirical fits compared to the standard OC3 algorithms is their increased predicted Chla at high end (Fig. 3), the intersensor variability (MdAPE) between MODISA and VIIRS is slightly increased from 13.7% to 14.0% when using the coefficients fitted to *in situ* data (Table II). In order to improve the consistency between satellite sensors and at the same time keep them consistent with *in situ* datasets, we need an optimization that minimizes not only the differences between satellite and *in situ* match-ups but also the differences between the satellite estimates of different sensors [1]. The matching Rrs pairs of MODISA and VIIRS in $1° \times 1°$ subareas were further binned according to the corresponding $\log_{10}(\mathrm{MBR})$ value, which resulted in 89 "bracket points" of MODISA and VIIRS $\log_{10}(\mathrm{MBR})$ values. The differences in the derived Chla estimates were then minimized for the input vector consisting of 24 MODISA bracket points of MBR and Cins, 20 VIIRS bracket points of MBR and Cins, and 89 bracket points of MBR from MODISA and VIIRS. For this optimization, we used the trust-region method, a variant of the Levenberg–Marquardt method as implemented in the NMath numerical libraries (http://www.centerspace.net/). As a result, we produced two sets of polynomial coefficients (for both MODISA and VIIRS) of the MBR OC3 model called CALFIT2015 (Table III).

The optimization reduced the bias (MdRPE) between Chla derived with MODISA and VIIRS from -9.4% to practically zero (Table II and Fig. 4). It also reduced somewhat the scatter (MdUAPE) between MODISA and VIIRS from $\sim$14% to 10%. However, the other statistical indicators (R^2, rmse, and RmaSlope) were not improved.

IV. DISCUSSION

The resulting optimized Chla algorithm shows improved performance compared to the standard OC3 algorithm and

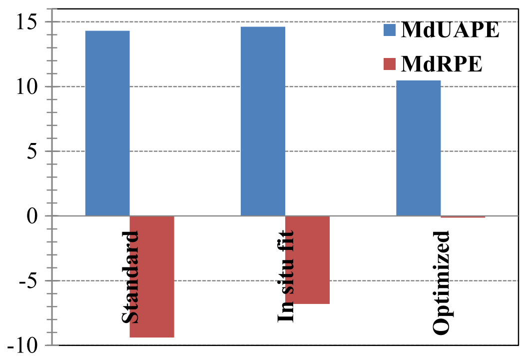

Fig. 4. Comparison of the differences between MODISA and VIIRS sensor-to-sensor match-ups: standard NASA *chlor_a* ("Standard"), empirical fit to the *in situ* Chla match-ups ("In situ fit"), and the optimized algorithm ("Optimized") showing the median unbiased percent error (MdUAPE) and the median relative percent error (MdRPE).

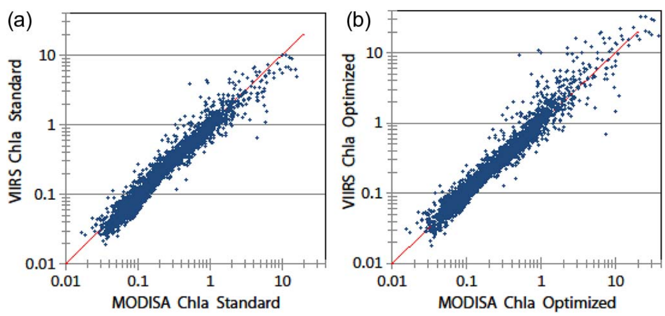

Fig. 5. VIIRS Chla versus MODISA Chla for a set of 4060 matching values of MBRs using the standard NASA *chlor_a* (a) and CALFIT2015 algorithm (b).

compared to the fit to *in situ* Chla match-ups. The observed underestimation of the standard OC3 algorithm at high *in situ* Chla was reduced, and the bias between Chla estimates by MODISA and VIIRS was eliminated (Table II and Fig. 4). The sensor-to-sensor scatter in Chla between MODISA and VIIRS was also somewhat reduced from 14% in the standard algorithm to 10% in the optimized algorithm. We also note that R^2, rmse, and RmaSlope of the VIIRS versus MODISA compatibility were not improved (Table II). This is explained by the fact that the main effect of fitting to *in situ* data was the increase in Chla estimates at high Chla levels (Figs. 3 and 5), but Rrs estimates corresponding to medium and high Chla are noisy [8]. Therefore, the scatter at high Chla was boosted, which inevitably made some of the statistics worse (e.g., rmse). As the median bias between MODISA and VIIRS has been eliminated, we can now merge Chla estimates from MODISA and VIIRS by simple arithmetic averaging of the gridded data and increase the frequency and spatial coverage and reduce uncertainty. However, we have to keep in mind that we have removed just the mean bias, and there may still exist bias between sensors related to factors such as sun zenith angle, sensor zenith angle, distance from the coast, etc. This has been discussed in [5] in the context of satellite-derived water clarity.

V. Conclusion

We have extended the optimization approach of [1] to current MODISA and VIIRS satellite data using a large database of *in situ* Chla and produced updated versions of the regionally optimized Chla algorithms. The new Chla estimates from MODISA and VIIRS are similar to standard *chlor_a* estimates at low Chla but have improved retrievals at medium to high *in situ* Chla and have no bias between one another. The improved algorithms (CALFIT2015) have been applied to MODISA and VIIRS imagery from 2012 to the present (2015). The merged satellite time series (available at http://spg.ucsd.edu/Satellite_Data/CC4km/CC4km.htm) have improved spatial and temporal coverage compared to a single sensor and improved correspondence to *in situ* data. Improved detection of high biomass events is crucial for running harmful algal bloom predictive models in coastal California that require accurate Rrs and chlorophyll values [10] and is also necessary to enhance our understanding of coastal biology and provide long-term continuity of ocean data records.

Acknowledgment

The authors would like to thank the CalCOFI program and Dr. R. Goericke for providing the *in situ* Chla data. Satellite data were provided by the NASA Ocean Color Processing Group.

References

[1] M. Kahru, R. M. Kudela, M. Manzano-Sarabia, and B. G. Mitchell, "Trends in the surface chlorophyll of the California Current: Merging data from multiple ocean color satellites," *Deep Sea Res. II, Top. Stud. Oceanogr.*, vol. 77–80, pp. 89–98, Nov. 2012.

[2] S. Maritorena and D. A. Siegel, "Consistent merging of satellite ocean color data sets using a bio-optical model," *Remote Sens. Environ.*, vol. 94, no. 4, pp. 429–440, Feb. 2005.

[3] W. W. Gregg, N. W. Casey, J. E. O'Reilly, and W. E. Esaias, "An empirical approach to ocean color data: Reducing bias and the need for post-launch radiometric re-calibration," *Remote Sens. Environ.*, vol. 113, no. 8, pp. 1598–1612, Aug. 2009.

[4] C. Hu and C. Le, "Ocean color continuity from VIIRS measurements over Tampa Bay," *IEEE Geosci. Remote Sens. Lett.*, vol. 11, no. 5, pp. 945–949, May 2014.

[5] B. B. Barnes and C. Hu, "Cross-sensor continuity of satellite-derived water clarity in the Gulf of Mexico: Insights into temporal aliasing and implications for long-term water clarity assessment," *IEEE Trans. Geosci. Remote Sens.*, vol. 53, no. 4, pp. 1761–1772, Apr. 2015.

[6] B. A. Franz, S. W. Bailey, J. P. Werdell, and C. R. McClain, "Sensor-independent approach to the vicarious calibration of satellite ocean color radiometry," *Appl. Opt.*, vol. 46, no. 22, pp. 5068–5082, Aug. 2007.

[7] C. Hu, L. Feng, and Z. Lee, "Uncertainties of SeaWiFS and MODIS remote sensing reflectance: Implications from clear water measurements," *Remote Sens. Environ.*, vol. 133, pp. 168–182, Jun. 2013.

[8] M. Kahru, R. M. Kudela, C. R. Anderson, M. Manzano-Sarabia, and B. G. Mitchell, "Evaluation of satellite retrievals of ocean chlorophyll-a in the California Current," *Remote Sens.*, vol. 6, no. 9, pp. 8524–8540, Sep. 2014.

[9] M. Szeto, J. P. Werdell, T. S. Moore, and J. W. Campbell, "Are the world's oceans optically different?" *J. Geophys. Res.*, vol. 116, no. C7, Jul. 2011, Art. ID. C00H04.

[10] C. R. Anderson *et al.*, "Detecting toxic diatom blooms from ocean color and a regional ocean model," *Geophys. Res. Lett.*, vol. 38, no. 4, Feb. 2011, Art. ID. L04603.

[11] M. D. Ohman and E. L. Venrick, "CalCOFI in a changing ocean," *Oceanography*, vol. 16, no. 3, pp. 76–85, 2003.

[12] J. E. O'Reilly *et al.*, "Ocean color chlorophyll algorithms for SeaWiFS," *J. Geophys. Res.*, vol. 103, no. C11, pp. 24 937–24 953, Oct. 1998.

[13] J. P. Werdell and S. W. Bailey, "An improved *in-situ* bio-optical data set for ocean color algorithm development and satellite data product validation," *Remote Sens. Environ.*, vol. 98, no. 1, pp. 122–140, Sep. 2005.

[14] S. W. Bailey and J. P. Werdell, "A multi-sensor approach for the on-orbit validation of ocean color satellite data products," *Remote Sens. Environ.*, vol. 102, no. 1/2, pp. 12–23, May 2006.